Available online at www.sciencedirect.com
ScienceDirect
Diamond & Related Materials 16 (2007) 196–201
DIAMOND AND RELATED MATERIALS
www.elsevier.com/locate/diamond

Synthesis of carbon nanosheets and carbon nanotubes by radio frequency plasma enhanced chemical vapor deposition

Mingyao Zhu [a], Jianjun Wang [b], Ronald A. Outlaw [b], Kun Hou [b], Dennis M. Manos [a,b], Brian C. Holloway [a,b,c,*]

[a] Physics Department, College of William and Mary, Williamsburg, VA, 23187-8795, United States
[b] Department of Applied Science, College of William and Mary, Williamsburg, VA, 23187-8795, United States
[c] Luna nanoWorks Division, Luna Innovations, 521 Bridge Street, Danville, VA, 24543, United States

Received 1 March 2006; received in revised form 3 May 2006; accepted 9 May 2006
Available online 10 July 2006

Abstract

Carbon nanosheets are a two-dimensional carbon nanostructure consisting of free-standing graphite sheets (~1 nm thick) which we deposit using an inductively coupled RF PECVD method. Our previous reports have shown that carbon nanosheets can be grown on a variety of substrates, without catalyst, and under various growth conditions. In this work we describe process details and plasma control parameters to permit rapid changeover from nanotube to nanosheet deposition in the same system. We present a thorough characterization of the nanosheet layer that is produced under these circumstances. We also propose plausible mechanisms to account for the different mode of layer growth leading to the observed topography and conformation of the nanosheets. The experimental evidence suggests that a combination of high plasma electron density and large atomic hydrogen density of the inductively coupled plasma is the reason for nanosheet formation.

Keywords: Nanostructures; Graphite; RF plasma enhanced CVD

1. Introduction

Since 1991, when carbon nanotubes were adequately characterized and described by Iijima [1], carbon nanotubes have been a very active research topic. A variety of methods of carbon nanotube deposition have been developed [2], including arc discharge, pulsed laser deposition, thermal chemical vapor deposition, and direct current, hot filament, microwave, and most importantly for this study, radio frequency (RF) plasma enhanced chemical vapor deposition (PECVD).

More recently, synthesis of two-dimensional (2-D) carbon nanostructures has been reported by several groups [3–10]. In the work reported in this paper, and in the work of the other groups, nanosheets are observed to curl into layers oriented approximately perpendicular to the substrate. Although the base of the layers is in good contact with the substrate, these layers have no auxiliary lateral support and are therefore often said to be "free-standing". Ando et al. [7], obtained petal-like graphite sheets as a by-product of a carbon nanotube synthesis through DC arc-discharge evaporation; Shang et al. [5], synthesized carbon nanoflakes by a hot filament CVD method; Wu et al. [4], and Chuang et al. [10], synthesized carbon nanowalls by a microwave PECVD method, and Hiramatsu et al. [8], reported fabrication of carbon nanowalls by capacitive PECVD assist by hydrogen radical injection. In contrast to the work reported here, all of the other reports describe 2-D free-standing carbon nanostructures that are more than 10 nm thick. Novoselov et al. [9], obtained atomically thin graphite films by mechanical exfoliation, but, again contrasting with this work, their films lie flat on the substrate surface and therefore would not be as useful for certain device purposes. We recently reported the synthesis of 2-D carbon nanosheet structures by an inductively coupled RF PECVD [3,6,11,12]. Unlike the other 2-D carbon nanostructures reported, the carbon nanosheets we synthesized are free from impurities (either catalyst and/or other allotropes of carbon), atomically thin, and free-standing.

* Corresponding author. Luna nanoWorks Division, Luna Innovations, 521 Bridge Street, Danville, VA, 24543, United States.
E-mail address: hollowayb@lunainnovations.com (B.C. Holloway).

0925-9635/$ - see front matter © 2006 Elsevier B.V. All rights reserved.
doi:10.1016/j.diamond.2006.05.007

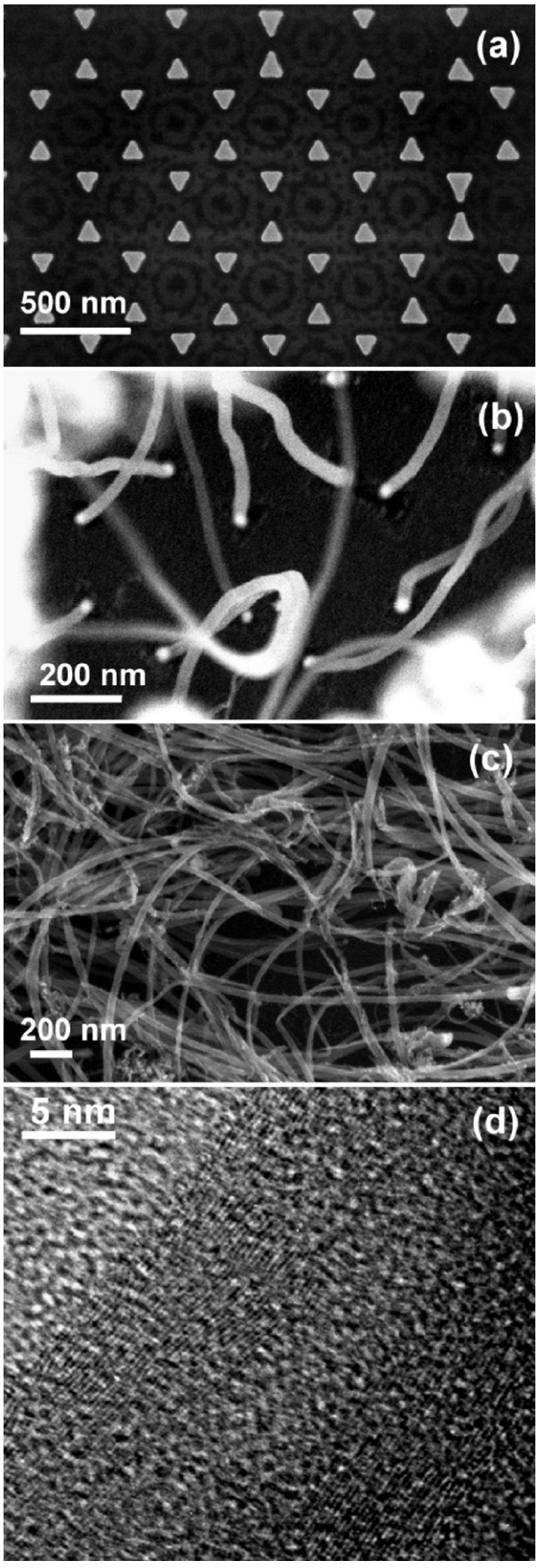

We have conducted depositions of both carbon nanotubes and carbon nanosheets in the same RF PECVD system by altering the process conditions. This has allowed us to investigate the comparative spatial and temporal growth of the two forms and led to a plausible mechanism for the formation of carbon nanosheets.

2. Experimental

In this study, carbon nanotubes and carbon nanosheets were grown in an RF PECVD system as detailed previously [6]. In brief, radio frequency (13.56 MHz) power was coupled into a vacuum chamber by a 3-turn coiled planar antenna through a quartz window on top of the chamber. By adjusting chamber pressure, and the RF magnitude and phases of the RF voltage and coil current in the coiled planar antenna configuration, either a capacitively or an inductively coupled plasma, or in some cases plasmas with some level of both characteristics, can be generated. The complete elimination of the capacitive component, often desirable to reduce sputtering from the coupling window, usually requires the addition of a Faraday shield. In this work we have been able to achieve such a result without the need for a shield, creating high-density inductively coupled plasma at lower pressure (~12 Pa for this study) and low-density capacitively coupled plasma at higher pressure (~130 Pa for this study).

A resistively heated sample stage was located 3.5 cm beneath the quartz window. The substrate temperature was monitored by a thermocouple at the upper surface of the substrates. The feedstock gases, including H_2, CH_4, NH_3, and C_2H_2, were introduced into the chamber through a side port and the gas flow rates were controlled by mass flow controllers.

A capacitive plasma was used for all nanotube depositions. Substrates for carbon nanotube depositions were (100) Si wafers with Ni catalyst patterned by a previously reported nanosphere lithography method [13] (see Fig. 1(a)). The substrates were pre-etched in an inductively coupled NH_3 plasma (8 sccm, ~12 Pa, 900 W RF power) for 5 min to optimize the catalyst dot size. The feedstock gases were typically 20% C_2H_2 (15 sccm) in NH_3 (60 sccm); and the total pressure was kept at 130 Pa by adjusting the pumping valve. The substrate temperature was 680 °C and the RF power was 700 W for the nanotube deposition. The deposition period was 25 min. The sample stage was grounded during the deposition so that the capacitive plasma was constrained between the sample stage and the quartz window.

Carbon nanosheets have been deposited under a variety of conditions in an inductively coupled plasma. Our observation is that they grow in our system without the need for any specific catalysts; indeed they can be grown on nearly any substrate of

Fig. 1. SEM images (a) of the Si substrates with Ni nanodots patterned by a nanosphere lithography method. SEM (b and c) and HRTEM (d) images of typical nanotubes deposited in a capacitive plasma of 20% C_2H_2 in NH_3. Other conditions are 700 W, ~130 Pa, 75 sccm, 680 °C, and 25 min for RF power, total pressure, total gas flow, substrate temperature, and deposition time. The substrates were pre-etched in an inductive NH_3 plasma (8 sccm, ~12 Pa, 900 W, and 5 min) before the deposition.

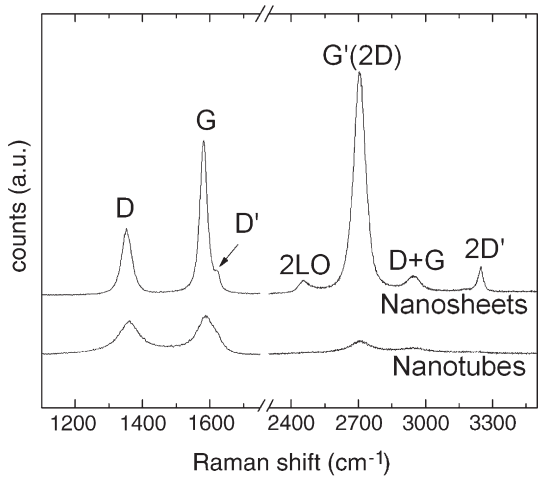

Fig. 2. Raman spectra of typical nanotube and typical nanosheet samples excited with 514 nm Ar^+ ion laser. The presence of the *D* and *G* peaks and *D′* shoulder for both the nanotube and nanosheet samples indicates that both have a defective graphitic structure. Second order peaks are also pronounced for nanosheet sample.

interest. In this work, nanosheets were grown on several choices of materials. The typical nanosheets were deposited with the substrate temperature of 680 °C; the feedstock was 40% CH_4 (4 sccm) in H_2 (6 sccm); the pressure was ~12 Pa and the RF power was 900 W. The deposition period was 20 min. Nickel grids and (100) Si wafers were used as substrates for electron microscopy imaging and Raman spectroscopy, respectively. The sample stage was usually electrically isolated, however, results from experiments not detailed here have shown that grounding the substrate during deposition does not affect the nanosheets produced.

In order to identify the critical parameters that drive nanosheet growth, three experimental variations were conducted to deposit carbon nanotubes under conditions similar to nanosheet growth and vice versa. First, carbon nanotubes were deposited using typical nanosheet feedstock (20% CH_4 in H_2) in a capacitive plasma (at 130 Pa pressure) for 5 min. For this experiment the substrates were pre-etched in an inductive hydrogen plasma for 5 min. Second, typical carbon nanosheets were deposited in an inductive plasma on Ni nanodot-patterned Si wafers (the same as those used for carbon nanotube deposition). Third, nanosheets were deposited using typical nanotube feedstock (20%–80% C_2H_2 in NH_3) in an inductive plasma on Ni nanodot-patterned Si wafers. In order to generate an inductive plasma for the third experiment, the total gas flow rate was 10 sccm so that the total pressure was ~12 Pa.

Morphology and structures of both the nanotube and nanosheet samples were investigated by scanning electron microscope (SEM, Hitachi S-4700), high resolution transmission electron microscope (HRTEM, Jeol JEM 2010F, 200 kV), and Raman spectroscopy (Renishaw, InVia, 514 nm Ar^+ laser excitation). Optical emission spectra (OES) of the plasma were collected by a fiber optic spectrometer (Ocean Optics, USB2000) to monitor the plasma species composition, emission intensity, and relative concentration.

3. Results and discussion

The results of the typical C_2H_2/NH_3 nanotube growth experiments are shown in Fig. 1. The Ni patterning on the Si substrate surface produced via nanosphere lithography [13] is shown in Fig. 1(a). The triangular features coalesce into nanodots upon heating/etching in the vacuum system [13]. As indicated by the hexagonal patterned Ni dots at the roots of the nanotubes in Fig. 1(b), typical nanotubes formed via a base growth mechanism. Fig. 1(c) shows that the nanotubes produced

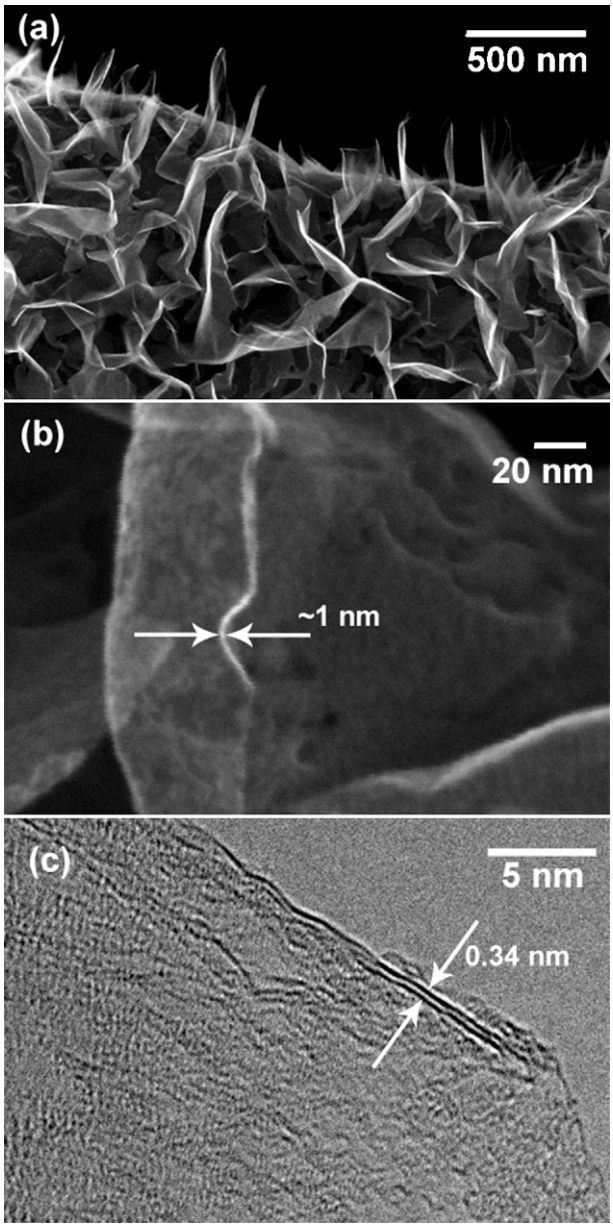

Fig. 3. (a) SEM image of typical nanosheets deposited on a Ni grid in order to show both plan and cross-section views in the same image. The nanosheets have a smooth surface morphology and are free-standing perpendicular to the substrate surface. (b) High magnification SEM image of one nanosheet edge with a thickness of ~1 nm. (c) HRTEM image of a single nanosheet; two parallel fringes at the fold-back location on the edge show that the sheet consists of only two graphene layers, and the distance between the two fringes is 0.34 nm.

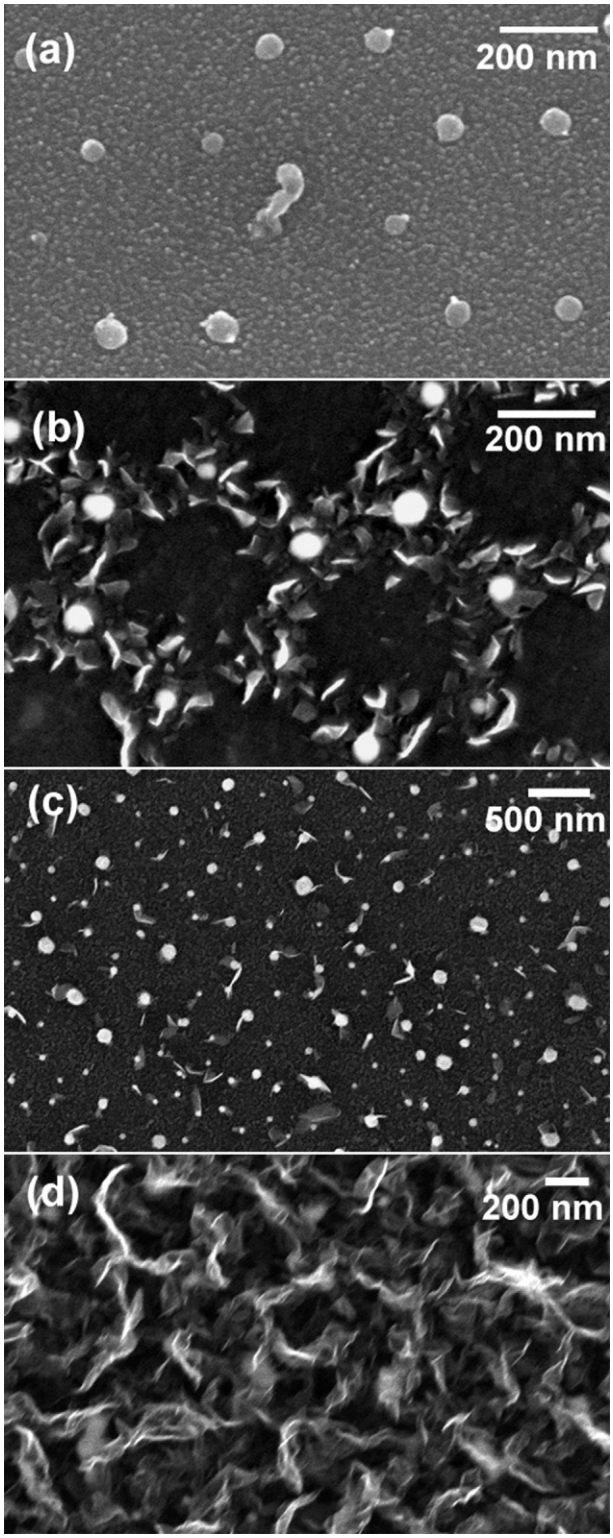

Fig. 4. SEM image (a) (30° tilted) of carbon nanofibers deposited in 20% CH_4/H_2 capacitive plasma at 130 Pa, 700 °C for 5 min on Ni nanodot-patterned Si substrate. SEM image (b) of carbon nanosheets was formed in 40% CH_4/H_2 inductive plasma at ~12 Pa for 5 min on the same type of substrate as in (a). Carbon nanosheets were deposited an inductive plasma with (c) 60% and (d) 80% C_2H_2 in NH_3 on Ni nanodot-patterned Si wafers; all other conditions are the same as for typical nanotube deposition. The nucleation density is extremely low at 20% and 40% C_2H_2, and increases for 60% C_2H_2 and complete coverage is achieved at 80% C_2H_2. Although more corrugated and defective, the C_2H_2/NH_3 nanostructures retain the sheet-like morphology.

are randomly oriented; 15–20 nm in diameter, and several microns in length. The HRTEM image in Fig. 1(d) indicates that they consist of parallel rolled graphene layers with a hollow center and the layers are parallel to the tube axis, so they truly are multi-walled nanotubes, not bamboo-like carbon nanofibers.

The Raman spectrum from a typical nanotube sample (Fig. 2) has a D peak, a G peak and a D' shoulder at ~1350 cm^{-1}, ~1580 cm^{-1}, and ~1620 cm^{-1}, respectively, which is representative for multi-walled carbon nanotubes. Fig. 2 also shows the Raman spectrum from a typical nanosheet sample which also has the same D, G, and D' peaks as well as more enhanced second order peaks. For a more detailed analysis of nanosheet Raman spectra the reader is referred to references [3,6].

Fig. 3(a) is a SEM image of typical (40% CH_4 in H_2) nanosheets grown on a Ni grid so both plan and cross-section views are presented (nanosheets grown on Si wafer have the same morphology and structure). The nanosheets have a smooth surface morphology and are free-standing nearly vertical to the substrates. Typical nanosheets are hundreds of nanometers wide and ~700 nm high, but, as shown in Fig. 3(b) and Ref. [3], they are 1 nm or less in thickness. The high resolution transmission electron micrograph, Fig. 3(c), shows a single nanosheet, consisting of 2 atomic layers at the curled edge and the inter-plane distance is 0.34 nm. As reported in reference [3], typical nanosheets have a graphitic electron diffraction pattern. As detailed in reference [11], the asymmetric X-ray diffraction pattern of typical nanosheets shows (002), (004) and (101) reflections, further confirming that nanosheets have a defective graphitic structure.

X-ray photoelectron spectroscopy and Auger electron spectroscopy results [14] indicate that carbon is the only element detected in typical nanosheets, with the exception of very small amounts of oxygen from adsorbed H_2O due to ambient exposure. Thermal desorption spectroscopy data [15] revealed that there is also a large amount ($2.375\times10^{17}/cm^{-2}$) of H atoms incorporated into ~600 nm high nanosheets deposited under typical conditions.

Fig. 4(a) shows the SEM image of carbon nanofibers deposited in CH_4/H_2 capacitive plasma for 5 min. In this

Table 1
Comparison of the experimental parameters for nanotube and nanosheet depositions

Parameters	CNT	CNS
Catalyst	Necessary	No effect
Plasma pre-etching	Yes	No effect
Deposition temp. (°C)	~700	~700
Gases composition	20% CH_4 in H_2; 20% C_2H_2 in NH_3	10–100% CH_4 in H_2; 20–80% C_2H_2 in NH_3
Pressure (Pa)	~130	~12
Plasma power (W)	700	400–1200
Plasma coupling mode	Capacitively coupled	Inductively coupled
Sample stage	Grounded	No effect

The ability to use similar non-plasma parameters to deposit both nanosheets and nanotubes suggests the plasma coupling mode is an important difference in the two growth processes.

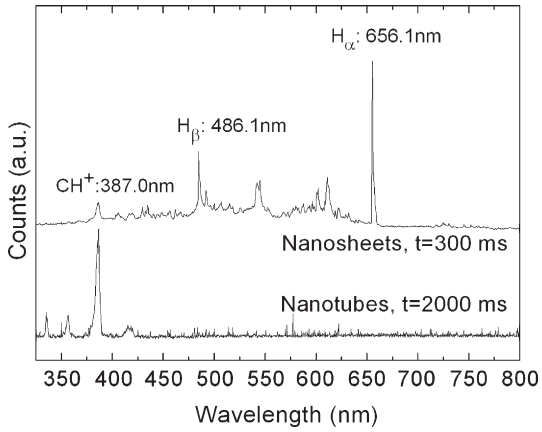

Fig. 5. Optical emission spectra of typical (C_2H_2/NH_3) capacitive nanotube plasma and typical (CH_4/H_2) inductive nanosheet plasma. The collection times were 2000 ms and 300 ms, respectively. The collection time was shortened for the inductive plasma to avoid detector saturation. For direct comparison the nanosheet spectrum should be multiplied by 6.7, which was not done in order to preserve the fine structure of the nanotube spectra.

experiment, the nanofiber density is extremely low because our system has been tuned away from the process window associated with carbon nanotube or nanofiber deposition. Thus the few nanofibers we create are not comparable to other high quality carbon nanotubes, such as those in DC [16] or hot filament PECVD [17]. Nevertheless, we note the appearance of 1-D carbon nanostructures, not 2-D nanosheets, that begin to form in the capacitive CH_4/H_2 plasma. Fig. 4(b) is a SEM image of the nanosheets deposited on a similar Ni patterned Si substrate in an inductive CH_4/H_2 plasma under typical nanosheet conditions for 5 min. Nanosheets have clearly nucleated and are growing around the Ni dots. Fig. 4(c) and (d) are nanosheets deposited on a Ni nanodot-patterned Si substrate in an inductively coupled plasma of 60% and 80% C_2H_2 in NH_3 with a constant total gas flow rate of 10 sccm and a total pressure of ~12 Pa at a substrate temperature of 680 °C for 5 min. The nanosheet nucleation density was extremely low at 20% and 40% C_2H_2 (not shown), but increased with higher C_2H_2 concentration. Although the nanosheets produced with C_2H_2 in NH_3 (Fig. 4(d)) are not as flat or smooth as typical nanosheets deposited from CH_4 in H_2 (Fig. 3(a)), they retain the same sheet-like morphology and are similar to CH_4/H_2 nanosheets deposited at a higher substrate temperature [6] and are consistent with XRD measurements which show a decreasing average uncorrugated length with increasing substrate temperature [11]. A detailed comparison of the parameters for nanotube and nanosheet deposition is listed in Table 1.

Using optical emission spectroscopy to compare typical deposition plasmas of the nanotubes and the nanosheets shows, as expected, that the inductive plasma produces a much higher density of atomic and molecular excited states. As shown in Fig. 5, the total optical emission intensity is much higher for the inductive plasma of typical nanosheet deposition as compared to the capacitive plasma of typical nanotube deposition. In addition, the atomic hydrogen peaks – H_α (656.1 nm) and H_β (486.1 nm) – are predominant for the nanosheet plasma, but do not rise above the noise for the nanotube plasma. It should be noted that the collection time for the inductive CH_4/H_2 plasma was reduced from 2000 ms to 300 ms to eliminate detector saturation. The spectra were not rescaled for direct comparison in order to preserve the fine structure of the nanotube plasma spectrum. Spectra from a capacitively coupled CH_4/H_2 plasma was collected but not shown, since the plasma was so dim that spectral features were too small to be distinguished from the ambient background.

On catalyst patterned substrates, carbon nanotubes were successfully synthesized in the capacitively coupled C_2H_2/NH_3 plasma. Synthesis of nanotubes from the capacitively coupled CH_4/H_2 plasma was not optimized, but nanotubes and/or nanofibers were formed (although of a low density). Chemical vapor deposition carbon nanotube and nanofiber growth mechanisms generally include dissolution, saturation and separation of carbon from the catalyst particles [18]. The catalyst is critical to the growth process, serving as a template of nucleation on which the nanotube forms. Efficient growth of carbon nanotube via CVD without catalyst is generally not possible.

However, no catalyst is needed for nanosheet deposition. In fact, nanosheets have been deposited on a variety of metallic, semiconducting and insulating substrates [3,6] without catalyst or special substrate preparation. Furthermore, as shown in Fig. 4 (b), (c) and (d), in an inductively coupled plasma nanosheets rather than nanotubes were deposited on Ni dots patterned silicon substrates at the same substrate temperature. This clearly indicates that nanosheet nucleation and growth are favorable over nanotube processes in an inductively coupled plasma deposition process. As listed in Table 1, all the conditions for nanotube and nanosheet deposition are the same except for the total pressure and thus the plasma coupling mode. This seems to be strong evidence that, although the fundamental mechanism for nanosheet growth is not yet clear, the plasma coupling mechanism is a critical factor.

Even though the gas pressure is usually ~10 times lower, the plasma density of an inductively coupled plasma is approximately 10 times higher than a capacitively coupled plasma because the fractional ionization rate is ~100 times higher due to the different coupling mechanisms [19]. During the inductively coupled plasma discharge for nanosheet deposition, the planar coil antenna acts as the primary inductance and the

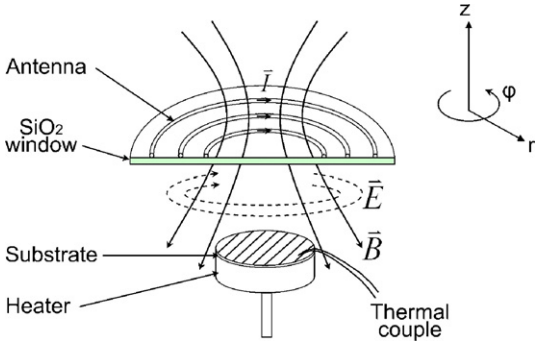

Fig. 6. Schematic of the configuration of the antenna and the distribution of the induced electromagnetic field in inductively coupled plasma in cylindrical coordinates as shown on right. The induced magnetic field is mainly in the $\vec{z}$ and $\vec{r}$ directions, thus the induced electric field is mainly in $\vec{\varphi}$ direction and thus is non-conservative.

discharging gas in the vacuum chamber acts as the secondary inductance, so the coupling force is the RF magnetic field. In the plasma, the coupled magnetic field has mainly $\vec{z}$ and $\vec{r}$ components, so the induced electric field has mainly $\vec{\varphi}$ component (as illustrated in Fig. 6) and is non-conservative, i.e. $\nabla \times E \neq 0$ [20], therefore charged particles can gain time-average energy from the field without collisions. This property fundamentally distinguishes a inductively coupled plasma from a capacitively coupled plasma which has conservative, irrotational electric fields. This increase in plasma density is consistent with the increase in atomic H and total emission signal seen in the optical emission spectra.

From the optical emission spectra in Fig. 5, it is clear that there is a dramatic increase in the intensity of the atomic hydrogen peaks from the inductive plasma used for typical nanosheet growth relative to the capacitive plasma used for nanotube growth. We believe the high relative concentration of atomic hydrogen in the plasma is one of the reasons for nanosheet formation. It is well known that atomic hydrogen plays an important role in diamond thin film growth [21,22] by etching amorphous carbon, sp^2 and sp^3 hybridized carbon at very different rates. We propose that in nanosheet deposition, atomic hydrogen prevents the formation of additional graphene layers by etching weakly bonded carbon atoms and small graphitic fragments. This is supported by the process conditions associated with 2-D carbon nanostructures reported in the literature, where the authors note that hydrogen appears to be a necessary process component [4,5,7,8]. Ando et al. [7], used H_2 in the DC arc-discharge evaporation to produce petal-like graphite sheets; Shang et al. [5], used 3–15% C_2H_2 in H_2 mixture in the hot filament CVD for the carbon nanoflake formation; Wu et al. [4], used 20% CH_4 in H_2 in the microwave PECVD for the carbon nanowall deposition and Hiramatsu et al. [8], used capacitive RF PECVD, however, assisted with a hydrogen radical injection for the carbon nanowall fabrication.

Our ongoing studies also suggest that the inductively coupled plasma may encourage nanosheet growth by providing higher concentration of activated carbon species and producing larger electric fields which may enhance the field-induced surface species migration. Further elaboration of the details of the mechanism of nanosheet formation is under investigation by our group.

4. Conclusion

Carbon nanosheets and nanotubes/nanofibers were successfully synthesized in the same RF PECVD system under almost the same condition with only different pressure and therefore different plasma coupling modes. One-dimensional nanotubes or nanofibers are formed in capacitively coupled plasma on catalyzed substrates. Although thicker nanosheet structures can be grown under other conditions, in our system, atomically thin, two-dimensional nanosheets are formed whenever the inductively coupled plasma mode dominates, even on patterned catalyst substrates and/or using a C_2H_2/NH_3 gas mixture. We attribute the growth of such extremely thin nanosheets, oriented nearly vertically with respect to the arbitrary choice of substrates, to a combination of high plasma density, high atomic hydrogen density and the presence of vertical electric fields at the substrate in the inductively coupled plasma.

Acknowledgment

The authors sincerely thank Ms. Kerry Siebein for her assistance with HRTEM at University of Florida, and the Office of Naval Research for funding (Grant No. N00014-02-1-0711).

References

[1] S. Iijima, Nature (London, United Kingdom) 354 (6348) (1991) 56.
[2] M.S. Dresselhaus, G. Dresselhaus, P. Avouris (Eds.), Carbon Nanotubes Synthesis, Structure, Properties, and Applications, Springer, 2001, 447 pp.
[3] J.J. Wang, M.Y. Zhu, R.A. Outlaw, X. Zhao, D.M. Manos, B.C. Holloway, V.P. Mammana, Applied Physics Letters 85 (7) (2004) 1265.
[4] Y.H. Wu, P.W. Qiao, T.C. Chong, Z.X. Shen, Advanced Materials 14 (1) (2002) 64.
[5] N.G. Shang, F.C.K. Au, X.M. Meng, C.S. Lee, I. Bello, S.T. Lee, Chemical Physics Letters 358 (2002) 187.
[6] J.J. Wang, M.Y. Zhu, R.A. Outlaw, X. Zhao, D.M. Manos, B.C. Holloway, Carbon 42 (14) (2004) 2867.
[7] Y. Ando, X. Zhao, M. Ohkohchi, Carbon 35 (1) (1997) 153.
[8] M. Hiramatsu, K. Shiji, H. Amano, M. Hori, Applied Physics Letters 84 (23) (2004) 4708.
[9] K.S. Novoselov, A.K. Geim, S.V. Morozov, D. Jiang, Y. Zhang, S.V. Dubonos, I.V. Grigorieva, A.A. Firsov, Science 306 (5296) (2004) 666.
[10] A.T.H. Chuang, B.O. Boskovic, J. Robertson. Diamond and Related Materials (in press).
[11] B.L. French, J.J. Wang, M.Y. Zhu, B.C. Holloway, Journal of Applied Physics 97 (11) (2005) 114317/1.
[12] B.L. French, J.J. Wang, M.Y. Zhu, B.C. Holloway, Thin Solid Films 494 (1–2) (2006) 105.
[13] J.J. Wang, M.Y. Zhu, X. Zhao, R.A. Outlaw, D.M. Manos, B.C. Holloway, C. Park, T. Anderson, V.P. Mammana, Journal of Vacuum Science and Technology, B 22 (3) (2004) 1269.
[14] J.J. Wang, M.Y. Zhu, H. Tian, X. Zhao, R.A. Outlaw, D.M. Manos, B.C. Holloway, Journal of Vacuum Science and Technology, B (submitted for publication).
[15] X. Zhao, R.A. Outlaw, J.J. Wang, M.Y. Zhu, G.D. Smith, B.C. Holloway, Journal of Chemical Physics 124 (2006) 194704.
[16] M. Chhowalla, K.B.K. Teo, C. Ducati, N.L. Rupesinghe, G.A.J. Amaratunga, A.C. Ferrari, D. Roy, J. Robertson, W.I. Milne, Journal of Applied Physics 90 (10) (2001) 5308.
[17] Z.P. Huang, D.L. Carnahan, J. Rybczynski, M. Giersig, M. Sennett, D.Z. Wang, J.G. Wen, K. Kempa, Z.F. Ren, Applied Physics Letters 82 (3) (2003) 460.
[18] T.W. Ebbesen (Ed.), Carbon Nanotubes: Preparation and Properties, 1997, 296 pp.
[19] M.A. Lieberman, A.J. Lichtenberg, Principles of Plasma Discharges and Materials Processing, John Wiley & Sons, Inc., New York, 1994. 572 pp.
[20] J. Hopwood, C.R. Guarnieri, S.J. Whitehair, J.J. Cuomo, Journal of Vacuum Science and Technology, A 11 (1) (1993) 147.
[21] J.A. Mucha, D.L. Flamm, D.E. Ibbotson, Journal of Applied Physics 65 (9) (1989) 3448.
[22] Y. Muranaka, H. Yamashita, K. Sato, H. Miyadera, Journal of Applied Physics 67 (10) (1990) 6247.